Hadronic contributions to the anomalous magnetic moment of the muon

T. Kinoshita, B. Nižić, and Y. Okamoto
Newman Laboratory of Nuclear Studies, Cornell University, Ithaca, New York 14853
(Received 10 September 1984)

We have evaluated the hadronic contribution to the muon anomaly arising from diagrams containing hadronic light-by-light scattering subdiagrams using two different models. Our result is $49(5)\times 10^{-11}$ which disagrees with an earlier calculation. We have also improved the contribution of the hadronic vacuum polarization diagrams to second- and fourth-order QED diagrams, using the latest experimental data. The results are $707(19)\times 10^{-10}$ and $-90(5)\times 10^{-11}$, respectively. The complete hadronic contribution is thus $703(19)\times 10^{-10}$. The remaining error comes predominantly from the experimental inputs needed for evaluating the hadronic vacuum polarization effect.

I. INTRODUCTION AND SUMMARY

The anomalous magnetic moment a_μ is one of the basic properties of the muon which is measurable with great precision and also calculable from theory. Thus it provides a sensitive tool for testing the validity of the theoretical framework. In early days it served as a testing ground of QED. More recently it has been used for detection of the hadronic vacuum polarization effect. It has also been used to impose constraints on the possible internal structure of the muon[1] and constraints on possible models for explaining the unexpected abundance of the radiative Z decay,[2] along with useful bounds on supersymmetric theories.[3]

The most accurate measurements of the muon anomaly thus far are those obtained at the CERN muon storage ring:[4]

$$a_{\mu^-}^{\exp}=11\,659\,370(120)\times 10^{-10}\,, \tag{1.1a}$$

$$a_{\mu^+}^{\exp}=11\,659\,110(110)\times 10^{-10}\,, \tag{1.1b}$$

where the numerals enclosed in parentheses represent the uncertainties in the final digits of the measured values. The best theoretical estimate reported prior to this article is[5,6]

$$a_\mu^{\rm th}=11\,659\,213(100)\times 10^{-10}\,, \tag{1.2}$$

in good agreement with (1.1).

While the electron anomaly is dominated by the QED effect, the muon anomaly is much more sensitive to physics at smaller distances because of the larger mass scale of the muon. Thus $a_\mu^{\rm th}$ of (1.2) has a substantial contribution ($\approx 7\times 10^{-8}$) from the hadronic effect. Even the effect of weak interaction is not negligible. In the Weinberg-Salam version of the theory the weak-interaction contribution to a_μ to one-loop order is[7]

$$a_\mu(\text{weak})=195(1)\times 10^{-11}\,. \tag{1.3}$$

Here we have used the latest information on the Weinberg angle and the lower bound for the Higgs boson mass.[8] The error in (1.3) is not to be taken too seriously, however, since the size of the two-loop contribution is not known at present. Note that the contribution (1.3) is only a factor 5 smaller than the present experimental error. This means that, if measurement of a_μ is improved by an order of magnitude, a_μ will provide an important testing ground of gauge theories of the electroweak interaction at the one-loop level, independent of processes such as muon decay, Cabbibo universality, $|\Delta S|=1$ semileptonic decays of neutral K particles, K_L-K_S mass difference, and mass shifts of W and Z bosons, which also require one-loop corrections for good fits.[9]

In order to realize such a test, however, it is necessary to improve not only the experimental error but also the theoretical error by an order of magnitude. The theoretical error in (1.2) comes mostly from the uncertainty in hadronic contributions, while it also contains a nonnegligible QED component. We have tried to improve both contributions substantially over the last three years. Our results are summarized in a recent publication.[10] In this article we report in detail the result of our work on the hadronic contribution to a_μ. It arises from two types of diagrams: Hadronic vacuum polarization diagrams and hadronic light-by-light scattering diagrams shown in Figs. 1 and 2, respectively. The dominant contribution, which also has the largest error, comes from the diagram of Fig. 1(a), and it is this error that is the most serious obstacle for further improvement on the theoretical side.

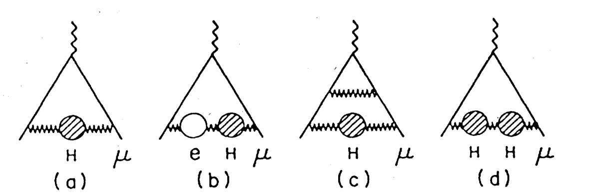

FIG. 1. Hadronic vacuum polarization contributions to a_μ. (a) Lowest-order hadronic vacuum polarization contribution to a_μ. (b) Hadronic vacuum polarization corrections to diagrams with an electron loop. There are two diagrams of this type. (c) An example of hadronic corrections to the fourth-order muon vertex diagram. There are 14 diagrams of this type. (d) Improper fourth-order hadronic vacuum polarization corrections to the second-order QED diagram.

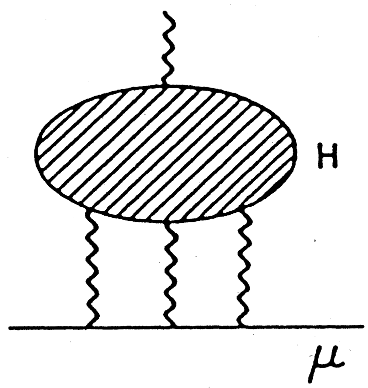

FIG. 2. Hadronic light-by-light scattering contributions to a_μ.

Nevertheless, it is very fortunate that this contribution to the muon anomaly can be evaluated without the knowledge of the underlying theory of strong interactions, owing to the fact that it can be directly related to the e^+e^- annihilation cross section measured in the colliding-beam experiment. Using the most recent experimental data, we have been able to improve the contribution to the muon anomaly due to the diagram of Fig. 1(a) to

$$a_\mu(\text{had}1a)=707(6)(17)\times10^{-10}\ , \tag{1.4}$$

where the first error is statistical and the second is systematic.[11] Here and throughout this paper we have used the ac Josephson value of the fine-structure constant:[12]

$$\alpha^{-1}=137.035\,963(15)\ . \tag{1.5}$$

We have also updated the results of Ref. 5 for the higher-order hadronic contributions to a_μ arising from the diagrams of Figs. 1(b), (c), and (d), using the same new data. Our results are

$$\begin{aligned} &a_\mu(\text{had}1b)=107(3)\times10^{-11}\ ,\\ &a_\mu(\text{had}1c)=-199(4)\times10^{-11}\ ,\\ &a_\mu(\text{had}1d)=2.3(0.6)\times10^{-11}\ . \end{aligned} \tag{1.6}$$

We have not included the contribution of Fig. 2(d) of Ref. 5, since we believe that it is already included in the evaluation of $a_\mu(\text{had}1a)$.

As for the hadronic light-by-light contribution, it is unfortunately not possible to use experimental data directly. Instead we have to evaluate this contribution using the theory of strong interactions. Although it is now commonly believed that quantum chromodynamics is the correct theory of strong interactions, it is powerless for the problem in question, since we are dealing here with the processes dominated by momenta of order m_μ where perturbative QCD is not expected to be reliable. Therefore, at present, the hadronic light-by-light contribution to the muon anomaly can be evaluated only in a model-dependent way. Such a calculation was attempted previously,[5] assuming that the blob in Fig. 2 can be approximated by quark loops of various flavors and colors. In view of the large error in the reported result $[-26(10)\times10^{-10}]$, we have reevaluated this contribution, using two different approaches. The first one is based on the same assumption as in Ref. 5 (except that the expansion in m_μ/m_q is not made). The second approach is based on the assumption that the blob in Fig. 2 can be approximated by charged pion loops and various low-energy resonances. Our results are

$$a_\mu(\text{had}2)=60(4)\times10^{-11}\ (\text{quark loop approximation}) \tag{1.7a}$$

$$=49(5)\times10^{-11}\ (\text{pion loop and resonances})\ , \tag{1.7b}$$

which are consistent with each other, but disagree strongly with the previous evaluation. (Note the difference in sign.) We believe that the disagreement is due to the poor convergence of numerical integration in Ref. 5. In the following we use (1.7b) rather than (1.7a), since (1.7a) is sensitive to the choice of quark mass. Since the magnitude of (1.7) is less than $\frac{1}{3}$ of the error of the dominant hadronic contribution (1.4), contrary to the previous result,[5] the uncertainty in (1.7) due to the model dependence will not affect our estimate of the overall hadronic contribution. Summing up the results (1.4), (1.6), and (1.7b), we find the total hadronic contribution to be

$$a_\mu(\text{hadron})=703(19)\times10^{-10}\ , \tag{1.8}$$

where we have combined statistical and systematic errors for simplicity.[11]

The present status of the QED contribution is

$$\begin{aligned} a_\mu(\text{QED})&=0.5\left[\frac{\alpha}{\pi}\right]+0.765\,858\,10(10)\left[\frac{\alpha}{\pi}\right]^2\\ &\quad+24.073(11)\left[\frac{\alpha}{\pi}\right]^3+140(6)\left[\frac{\alpha}{\pi}\right]^4\\ &=11\,658\,480(3)\times10^{-10}\ . \end{aligned} \tag{1.9}$$

Here the α^2 term is updated using the newest value of the muon mass, the α^3 term is improved by a reevaluation of the light-by-light term, and the α^4 term is evaluated for the first time. The details of these QED calculations are given in a separate paper.[13]

Summing up the contributions (1.3), (1.8), and (1.9), we obtain the new theoretical prediction[10]

$$a_\mu^{\text{th}}=11\,659\,203(20)\times10^{-10}\ , \tag{1.10}$$

in good agreement with the experimental value (1.1).

In summary, we should like to emphasize that the theoretical error of (1.10) is now down to the size comparable with the magnitude of the weak-interaction effect (1.3), bringing the latter within the range of laboratory detection. We believe that the error of (1.10) can be reduced further, in particular, in view of the novel approach to the measurement of $R(s)$ at CERN[14] which detects a $\pi^+\pi^-$ pair produced by a 300-GeV e^+ (from π^0 decay) incident on the e^-'s of target atoms. In this experiment, in which $\pi^+\pi^-$ and $\mu^+\mu^-$ pairs are counted simultaneously, $R(s)$ can be measured with an absolute accuracy of a few percent.

Thus far this experiment has reported measurements of $|F_\pi(q^2)|^2$ at $q^2=0.101$, 0.127, 0.152, and 0.178 $(\mathrm{GeV}/c)^2$ with an error of about 7%. This is a significant improvement over the previous results.[15] The new measurements are consistent with the dispersion-theoretical extrapolation whose parameters are determined predominantly by measurements at much larger q^2 where the accuracy is generally higher. For these reasons the values and errors of $a_\mu(\mathrm{had1})$, whether the new CERN data are included or not, are essentially unchanged at present. [The values (1.4) and (1.6) incorporate the data of Ref. 14.] Nevertheless, one should not overlook the significance of this experiment which marks an important step in freeing the evaluation of $a_\mu(\mathrm{had1})$ from any theoretical prejudice (however well founded that may be).

It will be clear from the above argument that a substantial improvement of $a_\mu(\mathrm{had1})$ by this technique requires measurements of $|F_\pi(q^2)|^2$ at larger q^2. It may be possible to explore it up to $q^2 \approx 0.35$ $(\mathrm{GeV}/c)^2$ at CERN SPS. The 1-TeV proton beam at Fermilab will extend the range to $q^2 \approx 1$ $(\mathrm{GeV}/c)^2$, well beyond the ρ, ω resonance region. If these experiments succeed and if further improvement is made in colliding-beam experiments, the theoretical error of a_μ will go down to 3×10^{-10} or less, removing a major obstacle for the experimental test of the electroweak effect (1.3). Thus, now appears to be the opportune time to launch a new measurement of a_μ designed to reduce the experimental error of (1.1) by at least an order of magnitude.[16]

The outline of this paper is as follows. In Sec. II we discuss the hadronic light-by-light contributions to a_μ using the picture in which the blob in Fig. 2 is approximated by quark loops of various colors and flavors. In Sec. III we present two versions of calculation of the hadronic light-by-light contribution to a_μ assuming that the hadronic blob in Fig. 2 can be approximated by pion loops and low-energy resonances. Hadronic structure effects are taken into account using the vector-meson-dominance model of photon. In Appendix A we discuss a new evaluation of the vacuum polarization contribution to a_μ. Some technical details concerning the parametric representation approach to theories with derivative coupling are given in Appendix B.

II. HADRONIC LIGHT-BY-LIGHT SCATTERING CONTRIBUTION TO a_μ. APPROXIMATING THE HADRONIC PART BY QUARK LOOPS

In this section we discuss the contribution to a_μ from the hadronic light-by-light scattering amplitude depicted in Fig. 2. Calmet *et al.*[5] obtained the result

$$a_\mu(\mathrm{had2}) = -26(10)\times10^{-10} \tag{2.1}$$

for this term, assuming that it is effectively given by the sum of quark loop contributions of various colors and flavors (see Fig. 3). Furthermore they assumed that quark masses m_q are larger than the muon mass m_μ so that an expansion in m_μ/m_q is justified. The result in (2.1) assumes the quark mass values of $m_u=m_d=0.3$, $m_s=0.5$, and $m_c=1.5$ GeV. The error of (2.1) is due to the numerical integration procedure only. It is not only the size of the error of (2.1) but also its negative sign that has attracted our attention to this contribution. This was rather unexpected since it is known[17] to be positive for $m_\mu/m_q=1$ (i.e., the contribution from the muon loop).

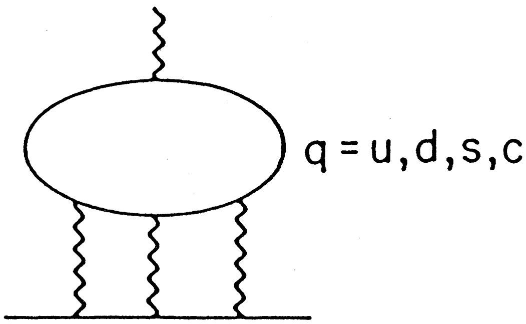

FIG. 3. Quark loop contributions to a_μ.

Let $a(m_\mu/m_q)$ be the naive quark loop contribution of Fig. 3 due to a quark of mass m_q and electric charge e_q. Then, adapting from pure QED calculation,[18] we can write

$$a(m_\mu/m_q=1)=0.370\,986(20)\times(3e_q{}^4)\times\left[\frac{\alpha}{\pi}\right]^3 . \tag{2.2}$$

For $e_q=\frac{2}{3}$ this is equal to 27.6×10^{-10}. Comparison of (2.1) and (2.2) raises two questions:

(i) Is it reasonable that $a(m_\mu/m_q)$ changes sign as $(m_\mu/m_q)^2$ decreases from 1 to 0.1?

(ii) Why is (2.1) of the same order of magnitude as (2.2) instead of being an order of magnitude smaller which would be the case if $a(m_\mu/m_q)$ behaves as $(m_\mu/m_q)^2$?

To answer these questions we have reexamined the contribution of Fig. 3. We started by integrating the exact expression, rather than the leading term of the expansion in m_μ/m_q as was done in Ref. 5, for the light-by-light contribution for various values of quark mass: $m_q=0.3$, 0.5, 1.5, 10, and 1000 (in GeV). Evaluation was made using the integration routine RIWIAD (Ref. 19) with the same number of hypercubes $(=2\times10^5)$ and the same number of iterations $(=7)$ for all m_q. In this manner we have been able to compare the speed of convergence of our integration procedure for various values of m_q. Since $a(m_\mu/m_q)$ will be approximately proportional to $(m_\mu/m_q)^2$, the product $(m_q/m_\mu)^2 a(m_\mu/m_q)$ will be roughly independent of m_μ/m_q. We list $(m_q/m_\mu)^2 a(m_\mu/m_q)$ for $e_q=1$ in Table I. As is seen clearly from this table, this quantity is positive and roughly constant for all values of m_q. It is also seen that the relative numerical accuracy deteriorates steadily as m_q increases, indicating that the value of this integral is a result of delicate cancellation between positive and negative contributions and the cancellation becomes more and more difficult as m_q increases. To verify this observation we have examined the behavior of the integrand analytically in the limit of large m_q. We have found that the integral

TABLE I. Values of $(m_q/m_\mu)^2 a(m_\mu/m_q)$ for $e_q=1$.

m_q (GeV)	$10^8(m_q/m_\mu)^2 a(m_\mu/m_q)$
0.3	1.91(0.13)
0.5	1.96(0.22)
1.5	2.18(0.47)
10	1.84(1.56)
1000	5.94(9.16)

contains various terms which behave as $(m_\mu/m_q)^2\ln(m_q/m_\mu)$ and regains the expected $(m_\mu/m_q)^2$ behavior only as a result of delicate cancellation of logarithmic terms from different parts of the integration domain. This means that the coefficient of $(m_\mu/m_q)^2$ in the expansion of $a(m_\mu/m_q)$, which is an integral over Feynman parameters, is not pointwise integrable contrary to the implicit assumption of Ref. 5, and hence cannot be evaluated reliably by a Monte Carlo procedure.

We have thus identified the cause of the problem in the evaluation of (2.1) and resolved it to our satisfaction. From Table I we can readily evaluate the contribution of the quark loop light-by-light contribution to the muon anomaly.

Assuming $m_u=m_d=0.3$ GeV, $m_s=0.5$ GeV, and $m_c=1.5$ GeV, we find

$$a(\text{had2})=60(4)\times10^{-11} \tag{1.7a}$$

which, as expected, is positive and substantially smaller than (2.1).

III. HADRONIC LIGHT-BY-LIGHT SCATTERING CONTRIBUTION TO a_μ. APPROXIMATING THE HADRONIC PART BY PION LOOPS AND RESONANCES

In the previous section we evaluated the correction to a_μ due to the hadronic light-by-light scattering amplitude, approximating the hadronic part by the sum of quark loops of various colors and flavors. There are, however, some problems with this approximation. First of all, the result depends strongly on m_q. Because of quark confinement, however, there is an ambiguity in the definition of the quark mass m_q. Second, the contribution (1.7a) is governed by the low-energy behavior of the virtual quark loop (whose typical momenta are of order m_μ). It is not clear to what extent this approximation represents the correct physical picture in the low-energy region.

In order to test the validity of the above approximation we have evaluated the same contribution in another picture in which we approximate the hadronic part of the diagram in Fig. 2 by a loop of the lightest hadron, pion, and various low-energy resonances. Since typical momenta of virtual photons attached to the hadron loop are of order m_μ, these photons are not hard enough to resolve the internal structure of the hadron. Therefore, to a reasonably good approximation, we may treat the pion as an elementary field and use scalar QED to describe the photon-pion interaction. Two versions of this treatment are discussed in Secs. III A and B. To make this picture more realistic we have also incorporated the vector-meson-dominance (VMD) approximation. This is discussed in Sec. III C. Finally, the contribution of resonances is discussed in Sec. III D.

A. Charged-pion-loop contribution—direct method

In this subsection we consider the hadronic light-by-light scattering contribution based on the picture in which the hadronic part in Fig. 2 is represented by charged pion loops. As was mentioned earlier, we treat the pion as an elementary field and use scalar QED to describe the pion-photon interaction.

There are altogether 21 Feynman diagrams that contribute to the lowest order light-by-light scattering amplitude in scalar QED. They are shown in Fig. 4. The total amplitude is given in terms of the fourth-rank vacuum polarization tensor $\Pi_{\nu\rho\lambda\sigma}(k_1,k_2,k_3,k_4)$, where $k_i, i=1,2,3,4$, are the momenta of photons attached to the pion loop and the Pauli-Villars regularization is understood. Because of gauge invariance we have

$$k_1^\nu\Pi_{\nu\rho\lambda\sigma}(k_1,k_2,k_3,k_4)=0\,, \tag{3.1a}$$

$$k_2^\rho\Pi_{\nu\rho\lambda\sigma}(k_1,k_2,k_3,k_4)=0,\ \text{etc.} \tag{3.1b}$$

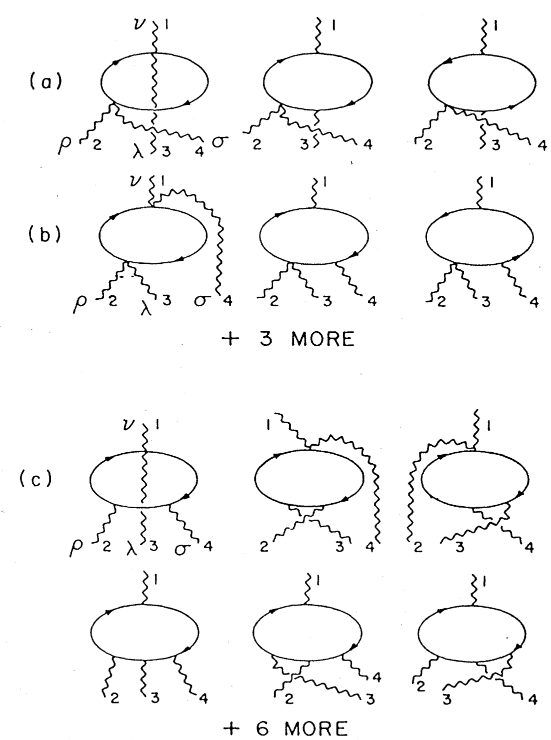

FIG. 4. Typical fourth-order diagrams contributing to the light-by-light scattering amplitude in scalar QED. There are 21 such diagrams altogether.

As is indicated in Fig. 4, the set of 21 Feynman diagrams can be classified into subsets, A, B, and C, comprised of 3, 6, and 12 diagrams, respectively, each being gauge-invariant with respect to photon 1. Relations (3.1a) hold for each of the three subsets separately. As a consequence of (3.1a) the total amplitude, as well as the partial amplitudes corresponding to the subsets A, B, and C, are finite, even though each contributing diagram is logarithmically divergent according to power counting.

Attaching the photon lines 2, 3, and 4 of these diagrams to the muon line, we obtain 21 sixth-order vertex diagrams. Charge-conjugation invariance (invariance under reversal of the direction of momentum flow in the pion loop) and time-reversal invariance reduce the number of independent diagrams to be evaluated to eight. They are shown in Fig. 5 together with the corresponding multiplicity factors which account for the diagrams related by the symmetries mentioned above.

To set up the Feynman integrals we make use of the Feynman-Dyson rules in parametric space described in Ref. 20. Note, however, that the parametric rules given in Ref. 20 must be modified slightly for theories with derivative coupling such as scalar QED. As is shown in Appendix B, the change to be made is

$$B'_{ij} \to B_{ij}$$

in Eq. (37) of Ref. 20(a). After this is done, one may proceed in the standard way.

Omitting the overall factor of $(\alpha/\pi)^3$, the amplitude corresponding to the diagram $\alpha(=A$ through $C)$ of Fig. 5 can be written, in the notation of Ref. 20, as

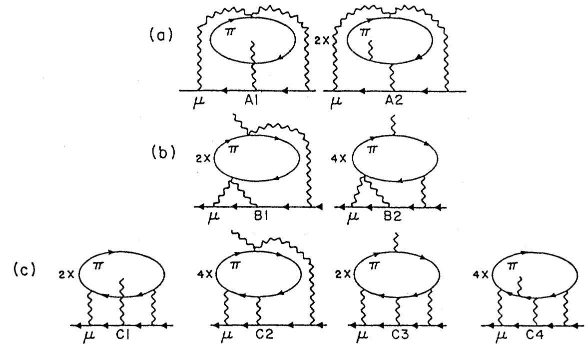

FIG. 5. Vertex diagrams containing scalar QED light-by-light scattering subdiagrams.

$$\Lambda_\alpha^\nu = -\tfrac{1}{16}F^\nu(D_i)\int(dz)\frac{1}{U^2V}, \quad \text{for } \alpha=A_1,B_1 ,$$

$$= -\tfrac{1}{32}F^\nu(D_i)\int(dz)\frac{1}{U^2V^2}, \quad \text{for } \alpha=A_2,B_2,C_1,C_2 ,$$

$$= -\tfrac{1}{32}F^\nu(D_i)\int(dz)\frac{1}{U^2V^3}, \quad \text{for } \alpha=C_3,C_4 . \tag{3.2}$$

These amplitudes have overall divergences and divergences associated with the corresponding light-by-light scattering subdiagram S_α. Projecting out the magnetic-moment term from (3.2), we find that the contribution to the muon anomaly arising from diagram α is of the form

$$M_\alpha = -\tfrac{1}{16}\int(dz)\frac{F_0}{U^2V}, \quad \text{for } \alpha=A_1,B_1 ,$$

$$= -\tfrac{1}{32}\int(dz)\left[\frac{F_0}{U^2V^2}-\frac{1}{2}\frac{F_1}{U^3V}\right], \quad \text{for } \alpha=A_2,B_2,C_1,C_2 ,$$

$$= -\tfrac{1}{32}\int(dz)\left[\frac{F_0}{U^2V^3}-\frac{1}{4}\frac{F_1}{U^3V^2}+\frac{1}{8}\frac{F_2}{U^4V}\right], \quad \text{for } \alpha=C_3,C_4 . \tag{3.3}$$

The details of the parametric functions U, V, F_0, F_1, and F_2 for each diagram in Fig. 5 are given in Ref. 21. F_0, F_1, and F_2 were obtained with the help of the algebraic manipulation routine SCHOONSCHIP (Ref. 22) (and in some cases by hand calculation).

The integral M_α depends logarithmically on the Pauli-Villars regularization mass of the light-by-light scattering subdiagram S_α. In this case, however, we can safely replace the regularization term by a term obtained by applying the K_S operation[20(b)] to the integrand of (3.3) without affecting the final result. The difference

$$\Delta M_\alpha = M_\alpha - K_{S_\alpha} M_\alpha \tag{3.4}$$

is now finite and can be evaluated numerically. The integral $K_{S_\alpha}M_\alpha$ factorizes as

$$K_{S_\alpha}M_\alpha = C_{S_\alpha} M_{\alpha/S_\alpha} , \tag{3.5}$$

where C_{S_α} is the overall divergent constant of subdiagram S_α, while M_{α/S_α} is the magnetic-moment term of the diagram α/S_α which is obtained from the diagram α by shrinking the subdiagram S_α to a point. ΔM_α in (3.4) represents the renormalized contribution to the muon anomaly arising from diagram α. The total contribution can then be written as

$$a_{HLL} = \sum_\alpha \eta_\alpha \Delta M_\alpha, \quad \alpha=A_1 \text{ through } C_4 , \tag{3.6}$$

where the multiplicative constants

$$\eta_\alpha = \begin{cases} 1, & \text{for } \alpha=A_1, \\ 2, & \text{for } \alpha=A_2,B_1,C_1,C_3, \\ 4, & \text{for } \alpha=B_2,C_2,C_4 , \end{cases} \tag{3.7}$$

TABLE II. Numerical results for various terms in (3.6).

Diagram	$\eta_\alpha \Delta M_\alpha$	Subcubes ($\times 10^5$)	Iterations
A_1	$-0.3927(5)$	5	31
A_2	$0.2767(6)$	5	35
B_1	$-0.4617(4)$	5	26
B_2	$0.1603(4)$	5	25
C_1	$0.4024(10)$	5	26
C_2	$0.8309(12)$	5	35
C_3	$-0.3017(10)$	5	13
C_4	$-0.5579(30)$	5	10

account for the time-reversal and charge-conjugation symmetries. Note that $\sum_\alpha \eta_\alpha C_{S_\alpha} M_{\alpha/S_\alpha}=0$ in contrast to the spinor QED case[23] where the corresponding sum is nonvanishing.

The results of numerical evaluation of individual integrals are summarized in Table II. The quoted uncertainties represent the 90% confidence limit estimated by the integration routine RIWIAD. By denoting the contributions arising from the gauge-invariant subsets $A+B$ and C as a_{HLL}^{A+B} and a_{HLL}^{C}, where A and B have been combined for convenience of comparison with (3.18), we find from Table II that

$$a_{HLL}^{A+B}=-0.4174(10)\left[\frac{\alpha}{\pi}\right]^3 \tag{3.8}$$

and

$$a_{HLL}^{C}=0.3737(35)\left[\frac{\alpha}{\pi}\right]^3 . \tag{3.9}$$

Adding (3.8) and (3.9), we find the total contribution to the muon anomaly due to the Feynman diagrams of Fig. 5 to be

$$a_{HLL}=-0.0437(36)\left[\frac{\alpha}{\pi}\right]^3 . \tag{3.10}$$

B. Charged-pion-loop contribution—alternative approach

As a check of the calculation presented in the previous subsection, we evaluate in this subsection the contribution of the same set of diagrams using a method based on the Ward-Takahashi identity.

Let us note, first of all, that the three gauge-invariant sets of vertex diagrams in Fig. 5 can be obtained from the self-energy diagrams shown in Fig. 6 by inserting an external vertex in the pion lines in all possible ways. As is well known, proper vertex and self-energy parts are related by the Ward-Takahashi identity

$$q_\mu \Lambda_G^\mu = \Sigma_G(p+q/2)-\Sigma_G(p-q/2) , \tag{3.11}$$

where Σ_G is calculated from self-energy diagram G and Λ_G is the sum of vertex diagrams obtained by inserting an external vertex in G in all possible ways. In our case all self-energy diagrams shown in Fig. 6 vanish by (generalized) Furry's theorem so that

$$q_\mu \Lambda_G^\mu(p,q)=0, \quad G=A,B,C . \tag{3.12}$$

Differentiating (3.12) with respect to q^ν and dropping terms quadratic and higher orders in q, we obtain

$$\Lambda_G^\nu(p,q\to 0)\approx -q_\mu \left[\frac{\partial \Lambda_G^\mu(p,q)}{\partial q_\nu}\right]_{q=0} . \tag{3.13}$$

Using the labeling of the momenta as in Fig. 7 and the gauge-invariance condition (3.1), the formula (3.13) for $G=A,B$ and C can be written as

$$\Lambda_G^\nu(p,q\to 0)\approx -ie^6\int \frac{d^4 r_1}{(2\pi)^4}\frac{d^4 r_2}{(2\pi)^4}\frac{1}{p_6{}^2}\frac{1}{p_7{}^2}\frac{1}{p_8{}^2}\frac{\gamma_\rho(\not p_4+m_\mu)\gamma_\lambda(\not p_5+m_\mu)\gamma_\sigma}{(p_4{}^2-m_\mu{}^2)(p_5{}^2-m_\mu{}^2)} q_\mu \left[\frac{\partial}{\partial q_\nu}\Pi_G^{\mu\rho\sigma\lambda}(-q,p_6,-p_7,-p_8)\right]_{q=0} . \tag{3.14}$$

Parametrizing (3.14) according to the method of Ref. 20 and projecting out the magnetic-moment term, we obtain an expression of the form

$$\begin{aligned} M_G &= -\tfrac{1}{16}\int (dz)\frac{F_0}{U^2 V} \quad \text{for } G=A,B ,\\ &= -\tfrac{1}{32}\int (dz)\left[\frac{F_0}{U^2V^2}-\frac{1}{2}\frac{F_1}{U^3V}\right], \quad \text{for } G=C . \end{aligned} \tag{3.15}$$

The details of the parametric functions appearing in (3.15) are given in Ref. 21. The algebraic manipulation was again performed with the help of SCHOONSCHIP. The integrals $M_G(G=A,B,C)$ are finite and ready for numerical integration. The total contribution to the muon anomaly due to the diagrams in Fig. 5 is given by

$$a_{HLL}=\sum_G \eta_G M_G , \tag{3.16}$$

where the summation is over all the self-energy diagrams of Fig. 6, and the multiplicative factors

$$\eta_G=\begin{cases}1, & \text{for } G=A,\\ 2, & \text{for } G=B,C,\end{cases} \tag{3.17}$$

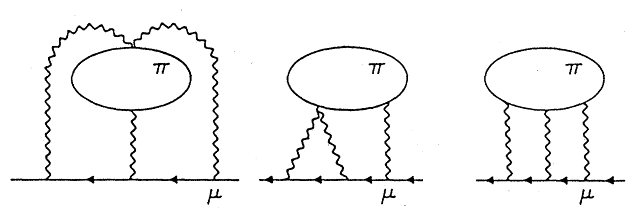

FIG. 6. Self-energy diagrams which correspond to the vertex diagrams of the gauge-invariant subgroups A, B, and C.

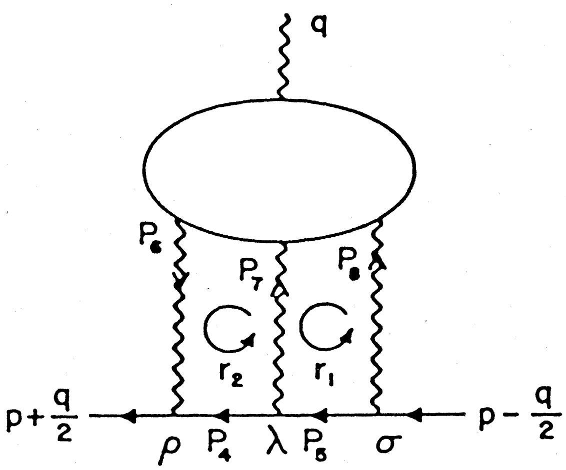

FIG. 7. A diagram indicating momentum labeling.

account for the time-reversal (for $G=B$) and charge-conjugation (for $G=C$) symmetries. Since the integrals M_A and M_B have similar structures [see (3.15)], they can be combined into one integral. Hence, the number of independent integrals is reduced from 8 (for the previous approach) to 2 (for the present approach), enabling us to save time and effort of computation. Evaluating these integrals numerically by RIWIAD, we find the following result for the joint contribution to the muon anomaly due to subgroups A and B:

$$a_{HLL}^{A+B} = -0.4155(9)\left[\frac{\alpha}{\pi}\right]^3, \tag{3.18}$$

while the contribution arising from the diagrams of subgroup C is

$$a_{HLL}^{C} = 0.3772(18)\left[\frac{\alpha}{\pi}\right]^3. \tag{3.19}$$

The numbers of subcubes used for numerical integration are 3×10^5 for the subgroups A and B, and 15×10^4 for the subgroup C. The numbers of iterations are 7 for the subgroups A and B, and 14 for the subgroup C. These results are in excellent agreement with the results (3.8) and (3.9) obtained in the previous subsection. Combining (3.18) and (3.19) we find the contribution to the muon anomaly coming from 21 Feynman diagrams of Fig. 5 to be

$$a_{HLL} = -0.0383(20)\left[\frac{\alpha}{\pi}\right]^3. \tag{3.20}$$

A slight disagreement between (3.20) and (3.10) is presumably caused by a delicateness of cancellation when separate contributions are put together.

C. Incorporating vector-meson-dominance picture

Our discussion thus far has been based on the usual scalar QED: We have been treating the pion as elementary. This treatment is not quite satisfactory in the sense that the pion, in fact, has structure. In principle the hadronic structure can be described by QCD. However, the momentum scale of our interest is small and the perturbative QCD does not apply here. The best available approximation to the actual hadronic picture at this energy scale will be the vector-meson-dominance (VMD) model. In VMD one assumes that hadrons are elementary but photon has hadronic structure; a photon transforms into a vector meson (such as ρ, ω, or ϕ) and the vector meson in turn couples to structureless hadrons. One benefit of VMD is that it provides a cutoff for momentum integration and makes resonance contributions to the muon anomaly, which are otherwise logarithmically divergent, finite as discussed in Sec. III D.

As the lowest-order approximation to the VMD picture, we take into account only the lowest-mass constituents of the photon (ρ^0 and ω). One of the diagrams contributing to a_μ in this picture is shown in Fig. 8. The coupling constants of the ρ meson to the pion and the photon are $-if_\rho$ and $igm_\rho{}^2$, respectively.[24] The ρ-photon line which connects the pion loop and the muon line in Fig. 8 can be written as

$$\frac{ef_\rho g m_\rho{}^2}{(p^2-m_\rho{}^2)p^2} = \frac{e^2}{p^2} - \frac{e^2}{p^2-m_\rho{}^2}. \tag{3.21}$$

Here we have used $g=e/f_\rho$ (Ref. 24). Thus the ρ-photon line splits into two terms: The first term is exactly the same as that in scalar QED without VMD, i.e., "bare photon" line, and the second term is the ρ line which provides a momentum cutoff to the scalar QED integral at the ρ mass. Therefore, we have to make only a slight modification to the original scalar QED integrals in order to obtain the integrals of the VMD model. Numerical evaluation by the integration routine VEGAS (Ref. 25) shows that the result for the subgroups A and B is changed to

$$a_{HLL}^{A+B} = -0.2703(12)\left[\frac{\alpha}{\pi}\right]^3, \tag{3.22}$$

while the result for the subgroup C becomes

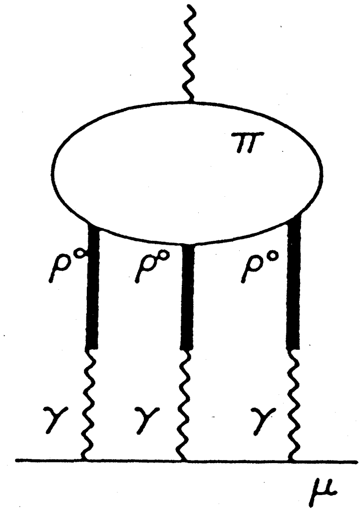

FIG. 8. A diagram with vector-meson insertions.

$$a^{C}_{HLL}=0.2578(15)\left[\frac{\alpha}{\pi}\right]^3 . \tag{3.23}$$

The numbers of subcubes used for numerical integration are 8×10^4 for the subgroups A and B, and 7×10^4 for the subgroup C. The numbers of iterations are 10 for both integrals. The quoted uncertainties again represent the 90% confidence limit estimated by the integration routine VEGAS.

Combining (3.22) and (3.23), we have the following contribution to the muon anomaly coming from the 21 Feynman diagrams of Fig. 5 in the VMD picture:

$$a_{HLL}=-0.0125(19)\left[\frac{\alpha}{\pi}\right]^3 . \tag{3.24}$$

We believe that this value is closer to reality than the values (3.10) and (3.20) obtained without proper attention to the extended structure of hadrons, and thus we will quote (3.24) instead of (3.10) or (3.20).

D. Resonance contributions

In this subsection we consider the contribution to the muon anomaly arising from various low-energy resonances. The contributing diagrams are depicted in Fig. 9. Let us start with the lowest mass resonance, π^0. The effective Lagrangian for the process $\pi^0\to2\gamma$ is given by

$$\mathscr{L}_{\pi^0\to2\gamma}=\frac{1}{\pi f_\pi}\alpha F_{\mu\nu}\tilde{F}^{\mu\nu} , \tag{3.25}$$

where $\tilde{F}^{\mu\nu}$ is the dual of $F^{\mu\nu}$, α is the fine-structure constant, and $f_\pi(=93$ MeV) is the pion-decay constant. The overall divergence of the integrals corresponding to the diagrams of Fig. 9 is removed by the magnetic-moment projection, but the integrals still contain logarithmic subdivergence, as can be seen by power counting. The vector-meson insertion (in the sense of VMD), however, provides the momentum cutoff and renders the integrals finite. The contribution of the diagram in Fig. 9(a) is given by an expression of the form

$$a_\mu^{\pi^0}[\text{Fig.9(a)}]=\left[\frac{m_\mu}{f_\pi}\right]^2\frac{-1}{64\pi^2}\int\frac{dz}{U^2}\times\left[\frac{B}{2U}\frac{1}{V}+\frac{C}{4U^2}\ln\tilde{V}\right] , \tag{3.26}$$

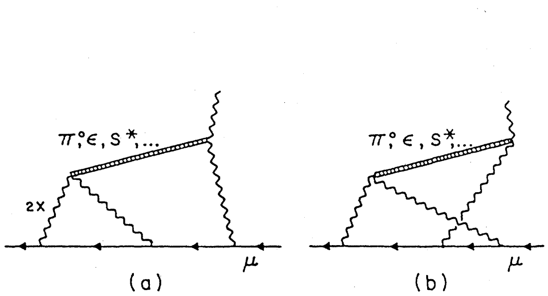

FIG. 9. Resonance diagrams contributing to the muon anomaly.

where U, V, $\tilde{V}$, and other parametric functions are given in Ref. 21. The contribution of the diagram in Fig. 9(b) is given by a similar expression. Evaluating these expressions numerically by VEGAS, we find

$$a_\mu(\pi^0)=0.052(5)\left[\frac{\alpha}{\pi}\right]^3 , \tag{3.27}$$

where the number of subcubes for the integrals is 16×10^3, and the number of iterations is 10.

Since the contribution to a_μ will decrease as the mass of resonance particle increases, we expect that higher mass resonance contributions to a_μ may be ignored compared to the contribution from the π^0 resonance (3.27). The next-lowest-mass resonances to be taken into account are the scalar resonances ϵ and S^* (at about 1 GeV). Using the effective Lagrangian density[26]

$$L_{\epsilon,S^*\to2\gamma}=-\sqrt{8\pi}\,\alpha(f\epsilon+f'S^*)F_{\mu\nu}F^{\mu\nu} , \tag{3.28}$$

where f (f') are coupling of ϵ (S^*) to the electromagnetic field, we find numerically

$$a_\mu(\epsilon)=0.13f^2a_\mu(\pi^0) \tag{3.29}$$

and

$$a_\mu(S^*)=0.13f'^2a_\mu(\pi^0) . \tag{3.30}$$

Since $f, f'\approx0.1$,[26] $a_\mu(\epsilon)$ and $a_\mu(S^*)$ are in fact negligible compared to $a_\mu(\pi^0)$. Contributions of the higher-mass resonances will be even smaller and may be ignored completely. Combining (3.24) and (3.27), we obtain the following contribution to the muon anomaly due to the pion loop and resonances:

$$a_\mu(\text{had}2)=49(5)\times10^{-11} , \tag{1.7b}$$

which is consistent with (1.7a), the result obtained using the quark-loop approximation. The error is our estimate of the model dependence (i.e., dependence on the cutoff m_ρ). Note that the π^0 resonance contribution (3.27) dominates (1.7b).

ACKNOWLEDGMENTS

We acknowledge the contribution of A. Garg who participated in the early phase of this work. We wish to thank Brookhaven National Laboratory and the National Laboratory for High Energy Physics (KEK), Japan, for generous support of our calculation. This work is supported in part by the National Science Foundation.

APPENDIX A: HADRONIC VACUUM POLARIZATION CORRECTIONS TO a_μ

In this appendix we give a new evaluation of the contribution to the muon anomaly due to the hadronic vacuum polarization diagram in Fig. 1(a). Previous estimates for this contribution are[5,27]

$$a_\mu(\text{had}1a)=660(100)\times10^{-10}$$
$$=702(80)\times10^{-10} . \tag{A1}$$

Using the most recent experimental data, we have updated this estimate to

$$a_\mu(\text{had}1a)=707(6)(17)\times10^{-10}\ , \tag{1.4}$$

where the first error is statistical and the second is systematic (see Table III). Note that the statistical error is more than 10 times smaller than the previous errors in (A1).

Let us now outline the calculation that has led to this result. As is well known this contribution can be written as[28]

$$a_\mu(\text{had}1a)=\frac{1}{4\pi^3}\int_{4m_\pi^2}^{\infty}ds\,\sigma_H(s)K(s)\ , \tag{A2}$$

where

$$K(s)=x^2\left[1-\frac{x^2}{2}\right]+(1+x)^2(1+x^{-2})\left[\ln(1+x)-x+\frac{x^2}{2}\right]+\frac{(1+x)}{(1-x)}x^2\ln x\ ,\quad x=\frac{1-(1-4m_\mu^2/s)^{1/2}}{1+(1-4m_\mu^2/s)^{1/2}}\ , \tag{A3}$$

and $\sigma_H(s)$ is the total cross section for e^+e^- annihilation into hadrons. Since $K(s)$ is a slowly varying function of s for most of s, the contribution to the integral (A2) comes mainly from $\sigma_{\text{tot}}(e^+e^-\to\pi^+\pi^-)$ in the low-energy region.

The $e^+e^-\to\pi^+\pi^-$ cross section in this energy range can be expressed in terms of the pion form factor $F_\pi(s)$ as

$$\sigma(e^+e^-\to\pi^+\pi^-)=\frac{8\pi}{3}\frac{\alpha^2q^3}{s^{5/2}}\,|F_\pi(s)|^2\ , \tag{A4}$$

where

$$q=\left[\frac{s}{4}-m_\pi^2\right]^{1/2}.$$

Taking account of the ρ-ω resonances, we can parametrize $F_\pi(s)$ using the modified Gounaris-Sakurai (GS) formula[29,30]

$$F_\pi=\left[\frac{A_1-m_\pi^2A_2}{A_1+A_2q^2+f(s)}+A_3e^{iA_4}\frac{m_\omega^2}{s-m_\omega^2+im_\omega\Gamma_\omega}\right]G(s)\ , \tag{A5}$$

where

$$f(s)=\frac{1}{\pi}\left[m_\pi^2-\frac{s}{3}\right]+\frac{2}{\pi}\frac{q^3}{\sqrt{s}}\ln\left[\frac{\sqrt{s}+2q}{2m_\pi}\right]-i\frac{q^3}{\sqrt{s}}\ , \tag{A6}$$

$$G(s)=\left[\frac{M^2}{s-M^2+iM\Gamma}\right]^n. \tag{A7}$$

In (A7) only the real part is kept for $\sqrt{s}<m_\pi+m_\omega$. The first term in the brackets in (A5) is the standard Gounaris-Sakurai formula.[31] The second term accounts for the ρ-ω interference.[32] The factor $G(s)$ was introduced by Quenzer *et al.*[29] to incorporate the effects of the ρ-ω inelastic channel. We take $M=1.2$ GeV, $\Gamma=0.15$ GeV, and $n=0.22$.[29] Using the data for $|F_\pi|^2$ from Refs. 14, 29, 33, 34, and 35, we have obtained the following mean values for the fitting parameters:

$$A_1=0.290(2)(\text{GeV})^2,\quad A_2=-2.30(1)\ ,\qquad A_3=-0.012(1),\quad\text{and } A_4=1.84(9)\ . \tag{A8}$$

The χ^2 is 175.7 with 95 degrees of freedom. The integration region was taken to be $2m_\pi\le\sqrt{s}\le1.1976$ GeV. The statistical error from this region has been evaluated by the formula

$$\sigma^2=\sum_{i,j}P_iH_{ij}P_j\ , \tag{A9}$$

where $P_i=\partial a_\mu/\partial A_i$ and H_{ij} is the covariance matrix. The systematic error in the measurement of $|F_\pi(s)|^2$ in this region is about 2%.[14,29,33,34] It is, however, not clear, especially after fitting the parameters, how the systematic error of a_μ depends on those of the experimental data for $|F_\pi(s)|^2$. In order to get some feeling we have evaluated (A2) in the same energy range by simply joining the data points of $\sigma_H(s)$ by straight lines, i.e., the trapezoidal rule. From the deviation of the mean values of a_μ in the two methods, we estimate the systematic error to be about 3%. The result is listed in Table III. Note that the second method is completely devoid of the dispersion-theoretical bias.

The ω resonance and ϕ resonance are treated by the Breit-Wigner formula

$$\sigma_{\text{BW}}=\frac{3\pi}{s}\frac{\Gamma_{\text{tot}}\Gamma_{e^+e^-}}{(\sqrt{s}-M_R)^2+\dfrac{\Gamma_{\text{tot}}^2}{4}}\ , \tag{A10}$$

where M_R is the mass of ω or ϕ, Γ_{tot} is the total width of ω or ϕ, and $\Gamma_{e^+e^-}$ is the partial width of ω or ϕ decaying into an e^+e^- pair. The statistical error was estimated using the statistical errors in the measurements of Γ_{tot} and $\Gamma_{e^+e^-}$. The systematic error is again somewhat unclear. We use 3.2% which is the systematic error in the measurements of Γ_{tot} and $\Gamma_{e^+e^-}$ (Ref. 36).

The other resonances have been treated using a narrow width approximation identical to the one used by Barger *et al.*[27] The error estimates are made in the same way as for the ω and ρ resonances.

The background contribution to (A2) from the region 1.1976 GeV$\le\sqrt{s}\le30.8$ GeV has been evaluated by the trapezoidal rule, using the experimental data for R, where

$$R(s)=\frac{\sigma_{\text{tot}}(e^+e^-\to\text{hadrons})}{\sigma(e^+e^-\to\mu^+\mu^-)}\ . \tag{A11}$$

This treatment is permissible because the background R is more or less constant (i.e., $\approx3\sum e_q^2$) for most of s. Since a_μ depends on R linearly [see (A2)], we can estimate the systematic error of a_μ by that of the measurement of R.

TABLE III. Hadronic contributions to the muon anomalous magnetic moment arising from Fig. 1(a). The first error is statistical and the second is systematic.

Contributing process and energy range	Contribution to $10^{10}a_\mu$	Reference
$\rho,\omega\to\pi^+\pi^-$ ($2m_\pi\le\sqrt{s}\le 1.1976$ GeV)	506.39(2.15)(15.0)	14,29,33,34,35
$\omega\to 3\pi$ ($3m_\pi\le\sqrt{s}\le 2.0$ GeV)	46.64(4.75)(1.49)	36
ϕ ($3m_\pi\le\sqrt{s}\le 2.0$ GeV)	40.17(1.80)(1.29)	36
$J/\psi(3.100)$	5.64(71)(85)	37
$\psi(3.685)$	1.47(21)(22)	37
$\psi(3.770)$	0.18(4)(4)	36
$\Upsilon,\Upsilon',\Upsilon'',\Upsilon'''$	0.085(3)(5)	38
	Background	
$e^+e^-\to\pi^+\pi^-$ ($1.1976\le\sqrt{s}\le 3.0$ GeV)	3.05(28)(31)	33,39
$e^+e^-\to\pi^+\pi^-\pi^0$ ($0.8432\le\sqrt{s}\le 1.002$ GeV)	2.92(81)(<81)	40
$e^+e^-\to K^+K^-$ ($1.05\le\sqrt{s}\le 3.0$ GeV)	4.32(32)(46)	33,34,41,42
$e^+e^-\to K_S{}^0K_L{}^0$ ($1.088\le\sqrt{s}\le 2.15$ GeV)	0.98(47)(10)	34,43,44
$e^+e^-\to p\bar{p}$ ($1.9\le\sqrt{s}\le 2.2375$ GeV)	0.17(3)(<3)	41,45
$e^+e^-\to\pi^+\pi^-\pi^0$ ($1.42\le\sqrt{s}\le 2.05$ GeV)	0.96(7)(10)	41
$e^+e^-\to K_S{}^0K^\pm\pi^\mp$ ($1.4415\le\sqrt{s}\le 2.05$ GeV)	1.12(9)(<9)	46
$e^+e^-\to\pi^+\pi^-\pi^0\pi^0$ ($0.99\le\sqrt{s}\le 2.05$ GeV)	23.95(79)(3.00)	47
$e^+e^-\to\pi^+\pi^-\pi^+\pi^-$ ($0.986\le\sqrt{s}\le 2.05$ GeV)	14.02(35)(1.12)	34,41,47
$e^+e^-\to K^+K^-\pi^+\pi^-$ ($1.45\le\sqrt{s}\le 2.05$ GeV)	1.39(9)(18)	48
$e^+e^-\to\pi^+\pi^-\pi^+\pi^-\pi^0$ ($1.202\le\sqrt{s}\le 2.05$ GeV)	1.75(15)(21)	34,49
$e^+e^-\to\pi^+\pi^-\pi^+\pi^-\pi^0\pi^0$ ($1.44\le\sqrt{s}\le 2.05$ GeV)	5.05(46)(1.00)	50
$e^+e^-\to\pi^+\pi^-\pi^+\pi^-\pi^+\pi^-$ ($1.45\le\sqrt{s}\le 2.05$ GeV)	0.43(4)(12)	51
$e^+e^-\to$ more than two hadrons ($2.05\le\sqrt{s}\le 3.15$ GeV)	21.63(81)(4.33)	52
$e^+e^-\to$ hadrons		
($3.15\le\sqrt{s}\le 7.8$ GeV)	19.81(27)(2.77)	53
($7.8\le\sqrt{s}\le 30.8$ GeV)	4.27(26)(26)	54
($\sqrt{s}\ge 30.8$ GeV) (Asymptotic freedom with 6 quarks)	0.4	
Total	706.8(5.9)(16.4)[a]	

[a]The second error is obtained by treating systematic errors by the least-squares method. Simple addition of these errors will give a value of about 34.

Note that for the contributions from the processes $e^+e^-\to\pi^+\pi^-\pi^0$ (0.8432 GeV $\le\sqrt{s}\le$ 1.002 GeV), and $e^+e^-\to K^+K^-$ (1.05 GeV $\le\sqrt{s}\le$ 3.0 GeV), we have subtracted the Breit-Wigner tails of ω and ϕ resonances, and the ϕ resonance itself, respectively, in order to avoid double counting. Finally, the contribution from the region $\sqrt{s}\ge 30.8$ GeV was estimated by the lowest-order QCD with six quarks. The results are summarized in Table III. The total contribution from this diagram [Fig. 1(a)] is given by (1.4).

APPENDIX B: CLARIFICATION OF THE PARAMETRIC METHOD IN THEORIES WITH DERIVATIVE COUPLING

In this appendix we present a minor simplification of the parametric method in theories with derivative coupling (e.g., scalar QED, QCD, etc.).

Given a Feynman diagram G with N internal lines, the Feynman-Dyson rules generate an integral of the form

$$M=\int \prod_{s=1}^{n} dr_s \frac{F(p_i)}{\prod_{i=1}^{N}(p_i{}^2-m_i{}^2)} , \tag{B1}$$

where m_i is the mass of the line i, n is the number of independent integration loops, r_s is the loop momentum, and $F(p_i)$ is a polynomial in the line momenta $p_1, p_2, \ldots, p_N$. Following the method of Ref. 20, we decompose the momentum of the line i as

$$p_i=q_i+k_i , \tag{B2}$$

where q_i is a linear combination of external momenta and k_i is the sum of loop momenta flowing in the line i. Next we replace p_i^μ in the numerator function $F(p_i)$ by the operator

$$D_i^\mu=\tfrac{1}{2}\int_{m_i{}^2}^{\infty} dm_i{}^2 \frac{\partial}{\partial q_i^\mu} . \tag{B3}$$

For example, for $F(p_i)=p_i^\mu$, we have

$$\frac{p_i^\mu}{\prod_{j=1}^{N}(p_j{}^2-m_j{}^2)}=D_i^\mu \frac{1}{\prod_{j=1}^{N}(p_j{}^2-m_j{}^2)} . \tag{B4}$$

This replacement of p_i^μ by D_i^μ can be extended to products of p_i^μ's as long as $F(p_i)$ contains no product of the form $p_i^\mu p_i^\nu \cdots$ (all p_i referring to the same line), which is the case for ordinary spinor QED. However, products of this type appear in scalar QED and other theories with derivative coupling. Terms of the form $p_i^\mu p_i^\nu \cdots$ require special care because after the first application of D_i, the second D_i acts not only on the denominator $\prod_{j=1}^{N}(p_j{}^2-m_j{}^2)$, but also on the numerator $p_i(=q_i+k_i)$, producing an extra term. How to handle this situation can be found in Ref. 20(c) [see Eq. (6.5) of Ref. 20(c)]. Namely, use

$$\frac{p_i^\mu p_i^\nu}{(p_i{}^2-m_i{}^2)^2}=D_i^\mu D_i^\nu \frac{1}{(p_i{}^2-m_i{}^2)^2}+\frac{g^{\mu\nu}}{2(p_i{}^2-m_i{}^2)} , \tag{B5}$$

or its generalization, and apply the parametric rules of Ref. 20(a). In fact, the second term in (B5) leads to a slight simplification of the parametric method. Namely, in Eq. (37) of Ref. 20(a) which reads

$$\begin{aligned} D_i^\mu \frac{1}{V^m}&=\frac{Q'^\mu_i}{V^m} , \\ D_i^\mu D_j^\nu \frac{1}{V^m}&=\frac{Q'^\mu_i Q'^\nu_j}{V^m}-\frac{1}{2(m-1)}\frac{B'_{ij}}{UV^{m-1}} , \quad \text{etc.} \end{aligned} \tag{B6}$$

use B_{ij} instead of B'_{ij}, where

$$B'_{ij}=B_{ij}-\delta_{ij}\frac{U}{z_i} \tag{B7}$$

[cf. Eq. (4) of Ref. 20(a)].

In order to show that this prescription is indeed correct, we present here a sample calculation of the pion self-energy diagram in scalar QED. The Feynman integral corresponding to the pion self-energy diagram is

$$M=-i(-ie)^2\int \frac{d^4r}{(2\pi)^4}\frac{g_{\mu\nu}(p_1+p_2)^\mu(p_1+p_2)^\nu}{(p_1{}^2-m_1{}^2)(p_2{}^2-m_2{}^2)} , \tag{B8}$$

where the indices 1 and 2 refer to pion and photon lines, respectively. In this integral the only term relevant for the present discussion is

$$I^{\mu\nu}=\int \frac{d^4r}{(2\pi)^4}\frac{p_1^\mu p_1^\nu}{(p_1{}^2-m_1{}^2)(p_2{}^2-m_2{}^2)} . \tag{B9}$$

Since the integral is quadratically divergent, we have to introduce two Feynman cutoffs to gain necessary powers of $1/V$ before we can apply the parametric rule. Then, taking (B5) into account, we find that

$$I^{\mu\nu}=\frac{i}{16\pi^2}\int (dz)\int_{m_\pi{}^2}^{\infty} z_1 dm_1{}^2 \int_0^\infty z_2 dm_2{}^2 \times \left[D_1^\mu D_1^\nu \frac{1}{U^2V^2} - \frac{g^{\mu\nu}}{2}\frac{1}{z_1U^2V} \right] . \tag{B10}$$

Here we have used Eqs. (19) and (31) of Ref. 20(a). Using (B6) and (B7), we find

$$D_1^\mu D_1^\nu \frac{1}{V^2}=\frac{Q'^\mu_1 Q'^\nu_1}{V^2}-\frac{g^{\mu\nu}}{2}\frac{B_{11}}{UV}+\frac{g^{\mu\nu}}{2}\frac{1}{z_1V} . \tag{B11}$$

Since the third term of (B11) and the last term of (B10) cancel each other, we have

$$I^{\mu\nu}=\frac{i}{16\pi^2}\int (dz)\int_{m_\pi{}^2}^{\infty} z_1 dm_1{}^2 \int_0^\infty z_2 dm_2{}^2 \times \left[\frac{Q'^\mu_1 Q'^\nu_1}{U^2V^2} - \frac{g^{\mu\nu}B_{11}}{2U^3V} \right] , \tag{B12}$$

which confirms our assertion.

[1]For a review of this subject see L. Lyons, in Prog. Part. Nucl. Phys. **10**, 227 (1983). See also F. M. Renard, Phys. Lett. **116B**, 264 (1982).

[2]F. del Aguila, A. Mendez, and R. Pascual, Phys. Lett. **140B**, 431 (1984).

[3]P. Fayet, in *Unification of the Fundamental Particle Interactions,* edited by S. Ferrara, J. Ellis, and P. van Nieuwenhuizen (Plenum, New York, 1980); J. A. Grifols and A. Mendez, Phys. Rev. D **26**, 1809 (1982); J. Ellis, J. Hagelin, and D. V. Nanopoulos, Phys. Lett. **116B**, 283 (1982); R. Barbieri and L. Maiani, *ibid.* **117B**, 203 (1982); D. A. Kosower, L. M. Krauss, and N. Sakai, *ibid.* **133B**, 305 (1983); T.-C. Yuan *et al.*, Northeastern University Report No. NUB 2633, 1984 (unpublished).

[4]J. Bailey *et al.*, Phys. Lett. **68B**, 191 (1977); F. J. M. Farley and E. Picasso, Ann. Rev. Nucl. Sci. **29**, 243 (1979).

[5]J. Calmet, S. Narison, M. Perrottet, and E. de Rafael, Phys. Lett. **61B**, 283 (1976); Rev. Mod. Phys. **49**, 21 (1977).

[6]C. Chlouber and M. A. Samuel, Phys. Rev. D **16**, 3596 (1977).

[7]R. Jackiw and S. Weinberg, Phys. Rev. D **5**, 2473 (1972); G. Altarelli, N. Cabibbo, and L. Maiani, Phys. Lett. **40B**, 415 (1972); I. Bars and M. Yoshimura, Phys. Rev. D **6**, 374 (1972); K. Fujikawa, B. W. Lee, and A. I. Sanda, *ibid.* **6**, 2923 (1972); W. A. Bardeen, R. Gastmans, and B. E. Lautrup, Nucl. Phys. **B46**, 319 (1972).

[8]W. Marciano, in *Proceedings of the 1983 International Symposium on Lepton and Photon Interactions at High Energies, Ithaca, New York,* edited by D. G. Cassel and D. L. Kreinick (Newman Laboratory of Nuclear Studies, Cornell University, Ithaca, 1984).

[9]See, for example, M. A. B. Beg and A. Sirlin, Phys. Rep. **88**, 1 (1982).

[10]T. Kinoshita, B. Nižić, and Y. Okamoto, Phys. Rev. Lett. **52**, 717 (1984).

[11]The systematic error in (1.4) is obtained by treating the systematic errors of Table III by the least-squares method. In view of the questionable nature of these errors, however, it may be more prudent to simply add them up, which yields the value 34×10^{-10}. In any case this problem cannot be settled until better measurements of the cross section for $e^+e^-\to$hadrons are made.

[12]E. R. Williams and P. T. Olsen, Phys. Rev. Lett. **42**, 1575 (1979).

[13]T. Kinoshita, B. Nižić, and Y. Okamoto (unpublished).

[14]S. R. Amendolia *et al.*, Phys. Lett. **138B**, 454 (1984).

[15]I. B. Vasserman *et al.*, Yad. Fiz. **30**, 999 (1979) [Sov. J. Nucl. Phys. **30**, 519 (1979)]; **33**, 709 (1981) [**33**, 368 (1981)].

[16]This may be achievable using high-intensity proton beams at the upgraded AGS or LAMPF II. See V. W. Hughes, in Proceedings of the Third LAMPF II Workshop, Los Alamos National Laboratory, 1983 (unpublished).

[17]J. Aldins, S. J. Brodsky, A. Dufner, and T. Kinoshita, Phys. Rev. D **1**, 2378 (1970).

[18]T. Engelman and M. J. Levine (unpublished).

[19]B. E. Lautrup, in *Proceedings of the Second Colloquium on Advanced Computing Methods in Theoretical Physics, Marseille, 1971,* edited by A. Visconti (University of Marseille, Marseille, 1971).

[20](a) P. Cvitanović and T. Kinoshita, Phys. Rev. D **10**, 3978 (1974); (b) **10**, 3991 (1974); (c) **10**, 4007 (1974).

[21]Y. Okamoto, Ph.D. thesis, Cornell University, 1984 (unpublished).

[22]H. Strubbe, Comput. Phys. Commun. **8**, 1 (1974); **18**, 1 (1979).

[23]T. Kinoshita and W. B. Lindquist, Cornell Report No. CLNS-81/509, 1981 (unpublished).

[24]See, for example, T. H. Bauer, R. D. Spital, D. R. Yennie, and F. M. Pipkin, Rev. Mod. Phys. **50**, 261 (1978).

[25]G. P. Lepage, J. Comp. Phys. **27**, 192 (1978); Cornell Report No. CLNS-447, 1980 (unpublished).

[26]G. Mennessier, Université des Sciences et Techniques du Languedoc report, 1981 (unpublished); Z. Phys. C **16**, 241 (1983).

[27]V. Barger, W. F. Long, and M. G. Olsson, Phys. Lett. **60B**, 89 (1975).

[28]M. Gourdin and E. de Rafael, Nucl. Phys. **B10**, 667 (1969); L. Durand, Phys. Rev. **128**, 441 (1962).

[29]A. Quenzer *et al.*, Phys. Lett. **76B**, 512 (1978).

[30]The expression in the large parentheses in (A5) corresponds to F_0^δ in $F_\pi=F_0^\delta G(s)$ in Ref. 29. Since they do not give an explicit expression for F_0^δ, we are not sure whether the two expressions are identical. Our fit of the data, however, is excellent, and we believe that the expression in (A5) represents a good parametrization.

[31]G. Gounaris and J. Sakurai, Phys. Rev. Lett. **21**, 244 (1968).

[32]M. Gourdin, L. Stodolski, and F. M. Renard, Phys. Lett. **30B**, 347 (1969).

[33]L. M. Kurdadze *et al.*, Novosibirsk Report No. IYF-82-97, 1982 (unpublished).

[34]G. V. Anikin *et al.*, *Proceedings of the 1983 International Symposium on Lepton and Photon Interactions at High Energies, Ithaca, New York* (Ref. 8). Our result (1.8) is at variance with the estimate made in this article. Unfortunately they give no details to allow a detailed comparison.

[35]I. B. Vasserman *et al.*, Yad. Fiz. **30**, 999 (1979) [Sov. J. Nucl. Phys. **30**, 519 (1979)]; **33**, 709 (1981) [**33**, 368 (1981)].

[36]Particle Data Group, Phys. Lett. **111B**, 1 (1982).

[37]G. J. Feldman and M. L. Perl, Phys. Rep. **33C**, 285 (1977).

[38]R. K. Plunkett, Ph.D. thesis, Cornell University, 1983 (unpublished).

[39]D. Bollini *et al.*, Lett. Nuovo Cimento **14**, 418 (1975).

[40]A. Cordier *et al.*, Nucl. Phys. **B172**, 13 (1980).

[41]J. E. Augustin *et al.*, in *Proceedings of the International Europhysics Conference on High Energy Physics,* Brighton, 1983, edited by J. Guy and C. Costain (Rutherford Appleton Laboratory, Chilton, Didcot, United Kingdom, 1983).

[42]B. Esposito *et al.*, Lett. Nuovo Cimento **28**, 337 (1980); B. Esposito *et al.*, Phys. Lett. **67B**, 239 (1977); M. Bernardini *et al.*, *ibid.* **46B**, 261 (1973).

[43]F. Mane *et al.*, Phys. Lett. **99B**, 261 (1981).

[44]P. M. Ivanov *et al.*, Pis'ma Zh. Eksp. Teor. Fiz. **36**, 91 (1982) [JETP Lett. **36**, 112 (1982)].

[45]G. Bassompierre *et al.*, Phys. Lett. **68B**, 477 (1977); B. Delcourt *et al.*, *ibid.* **86B**, 395 (1979).

[46]F. Mane *et al.*, Phys. Lett. **112B**, 178 (1982).

[47]V. Sidorov, in *Proceedings of the 1979 International Symposium on Lepton and Photon Interactions at High Energies,* edited by T. B. W. Kirk and H. D. I. Abarbanel (Fermilab, Batavia, 1979).

[48]A. Cordier *et al.*, Phys. Lett. **110B**, 335 (1982).

[49]A. Cordier *et al.*, Phys. Lett. **106B**, 155 (1981).

[50]M. Spinetti, in *Proceedings of the International Symposium on Lepton and Photon Interactions at High Energies* (Ref. 47).

[51]D. Bisello *et al.*, Phys. Lett. **107B**, 145 (1981).

[52]C. Bacci *et al.*, Phys. Lett. **86B**, 234 (1979).

[53]J. L. Siegrist, SLAC Report No. 225, 1979 (unpublished).

[54]L. Criegee and G. Knies, Phys. Rep. **83**, 151 (1982).